Antibacterial efficacy of antimicrobial peptide-functionalized hydrogel particles combined with vancomycin and oxacillin antibiotics

N.B. When citing this work, cite the original published paper.

(article starts on next page)

Antibacterial efficacy of antimicrobial peptide-functionalized hydrogel particles combined with vancomycin and oxacillin antibiotics

Annija Stepulane [a,c], Anand Kumar Rajasekharan [b], Martin Andersson [a,b,c,*]

[a] *Department of Chemistry and Chemical Engineering, Chalmers University of Technology, Gothenburg SE-412 96, Sweden*
[b] *Amferia AB, AZ BioVentureHub, Mölndal SE-431 83, Sweden*
[c] *Centre for Antibiotic Resistance Research in Gothenburg (CARe), SE-405 30 Gothenburg, Sweden*

ABSTRACT

The rise of antibiotic resistant bacteria, such as methicillin-resistant *Staphylococcus aureus* (MRSA), requires novel approaches to combat infections. Medical devices like implants and wound dressings are frequently used in conjunction with antibiotics, motivating the development of antibacterial biomaterials capable of exhibiting combined antibacterial effects with conventional antibiotics. This study explores the synergistic antibacterial effects of combining antimicrobial peptide (AMP) functionalized hydrogel particles with conventional antibiotics, vancomycin (VCM) and oxacillin (OXA), against *Staphylococcus aureus* and MRSA. The AMP employed, RRPRPRPRPWWWW-NH$_2$, has previously demonstrated broad-spectrum activity and enhanced stability when attached to hydrogel substrates. Here, checkerboard assays revealed additive and synergistic interactions between the free AMP and both VCM and OXA against *Staphylococcus aureus* and MRSA. Notably, the AMP-OXA combination displayed a significant synergistic effect against MRSA, with a 512-fold reduction in OXA's minimum inhibitory concentration (MIC) when combined with free AMP. The observed synergism against MRSA was retained upon covalent AMP immobilization onto the hydrogel particles; however, at a lower rate with a 64-fold reduction in OXA MIC. Despite this, the OXA-AMP hydrogel particle combinations retained considerable synergistic potential against MRSA, a strain resistant to OXA, highlighting the potential of AMP-functionalized materials for enhancing antibiotic efficacy. These findings underscore the importance of developing antimicrobial biomaterials for future medical devices to fight biomaterial-associated infections and reverse antimicrobial resistance.

1. Introduction

Antimicrobial peptides (AMPs) are a class of molecules that are part of the innate immune system of all multicellular organisms in the animal and plant kingdoms. Their antibacterial, antifungal, and antiviral properties have warranted significant research into using AMPs to fight infections (Zasloff, 2002; Yeung et al., 2011). Specific structural features, such as their positive charge and amphiphilic character as well as short amino acid chain length and secondary structure formation, have proven integral to the broad-spectrum antimicrobial activity of AMPs. Due to their positive charge, the predominant mode of action (MOA) of AMPs involves targeting membranes through interactions with the negatively charged cell membranes of microorganisms. These interactions disrupt membrane integrity, ultimately resulting in cell death.

Furthermore, additional MOAs have been reported, including the inhibition of protein, DNA and RNA synthesis as well as targeting of other intracellular sites (Bahar and Ren, 2013; Shai, 2002).

Due to the aforementioned reasons, AMPs have demonstrated broad-spectrum antibacterial activity against many Gram-positive, Gram-negative and multidrug-resistant (MDR) bacteria strains, that could be useful in antibacterial therapy. Given the increasing antibiotic resistance, AMPs are promising candidates over conventional antibiotics, as their nonspecific membrane-targeting is believed to result in reduced resistance, in contrast to the more target-specific intracellular MOAs of antibiotics (Yeung et al., 2011; Bahar and Ren, 2013). Additionally, AMPs have been investigated as adjuvants in combination with conventional antibiotics for combination therapy due to their synergistic interaction potential (Wu et al., 2021; Pizzolato-Cezar et al., 2019).

Drug synergism is defined as the combined effect of different drugs, where the resulting effect is greater than the sum of their individual effects (Lewies et al., 2017). Many AMPs have been investigated for their synergistic activity with antibiotics, where the bacterial membrane disruption is hypothesized to increase the bioavailability of the antibiotic, leading to enhanced potency, activity and even the reversal of antibiotic resistance (Lewies et al., 2017; Zharkova et al., 2019; Zhu et al., 2021; Sousa et al., 2021; Mhlongo et al., 2023). Furthermore, due to their excellent anti-biofilm properties, certain AMPs have shown great synergism with antibiotics for eradication of bacterial biofilms – precursors for biofilm-associated infections (Grassi et al., 2017; Reffuveille et al., 2014; Mataraci and Dosler, 2012; Li et al., 2022). Synergistic combinations of AMPs with antibiotics remain highly interesting research topics, due to benefits such as increased antibiotic potency at lower concentrations, enhanced clinical outcomes, reduced toxicity, prevention of resistance development and potential antibiotic repurposing (Mhlongo et al., 2023; Almaaytah et al., 2019).

Despite the promising antibacterial performance of AMPs, their low proteolytic stability and salt sensitivity pose a significant challenge for clinical translation, impacting their potential for use in combination therapy. To address issues associated with peptide stability, various stabilization methods have been proposed, ranging from AMP immobilization onto base materials to peptide delivery systems (Costa et al., 2011; Cesaro et al., 2023). Indeed, covalent immobilization of AMPs onto a material has demonstrated significant improvements in proteolytic stability and salt resistance, while retaining high antibacterial effect (Mishra et al., 2017; Costa et al., 2011; Blomstrand et al., 2022; Li et al., 2014). Therefore AMP-functionalized biomaterials have been developed for a range of medical devices, from biomedical implants to wound care products, as alternatives to traditional antibiotic therapy in the management of biomaterials-associated infections (Kazemzadeh-Narbat et al., 2021). By demonstrating broad-spectrum antibacterial activity both *in vitro* and *in vivo*, AMP-functionalized biomaterials offer significant potential for infection control through synergistic interactions with conventional antibiotics (Rai et al., 2022; Mishra et al., 2014; Cleophas et al., 2014; Atefyekta et al., 2021; Lim et al., 2013). While complete replacement of the use of antibiotics in biomaterials-associated infections management is unlikely, AMP-functionalized materials provide many potential synergistic benefits by combining antibiotic therapy with antibacterial materials.

Although numerous studies have been devoted to AMP-antibiotic combinations using AMPs in solution, i.e., their free soluble state, research on AMP-functionalized biomaterials in combination therapy with antibiotics remains sparse. A limited number of studies have primarily focused on AMP carrier materials in the form of drug delivery systems (Zarghami et al., 2021; Sharma et al., 2021; Orlando et al., 2008; Wang et al., 2020). Although these studies show promising antibacterial synergism, the low stability of AMPs remains an issue to be addressed. While these studies are indicative of the potential synergism between AMP-containing materials and antibiotics, to the best of our knowledge, interactions between covalently immobilized AMP materials and antibiotics have not been reported and remain an unexplored field of research. Therefore, combining covalently immobilized AMP materials with conventional antibiotics could offer the potential to harness the AMPs' broad-spectrum antibacterial activity along with increased antibiotic potency, reversal of resistance, and antibiotic repurposing for infection control.

In the present work, the potential synergism between a potent cationic AMP, RRPRPRPRPWWWW-NH$_2$ (RRP9W4N) covalently immobilized onto soft hydrogel particles in combination with conventional antibiotics, specifically VCM and OXA, against *S. aureus* and MRSA, was investigated. MRSA has emerged as a high priority pathogen where its common prevalence in hospital- and community-acquired infections, along with a lack of effective antibiotics strongly motivates the need for new antibacterial solutions (Tacconelli et al., 2018; Haque et al., 2018). RRP9W4N has been previously studied by our research

group, where AMP covalent immobilization onto hydrogel sheets and particles have resulted in materials with high antibacterial activity against *S. epidermidis*, *S. aureus*, *E. coli*, *P. aeruginosa*, MRSA, and MDR *E. coli*. These materials have potential applications in antibacterial wound dressings and coating materials, further motivating their synergistic combinations with conventional antibiotics for fighting biomaterial-associated infections and reversal of antimicrobial resistance (Atefyekta et al., 2021; Blomstrand et al., 2022; Stepulane et al., 2022; Blomstrand et al., 2023).

2. Materials and methods

2.1. Materials

Unless stated otherwise, all reagents used in this work were purchased from Sigma-Aldrich Sweden AB (Stockholm, Sweden) and used as received without further purification. Pluronic F127 diacrylate copolymer powder (Acr − PEO$_{100}$ − PPO$_{70}$ − PEO$_{100}$ − Acr, DA-F127) with a M$_w$ = 12600 g/mol and a purity of ≥95 % as well as AMP powder RRPRPRPRPWWWW-NH$_2$ (RRP9W4N) with M$_w$ = 1930 g/mol and purity of ≥90 % was provided by Amferia AB (Mölndal, Sweden). Ultrapure Milli-Q water was used for all steps of the material synthesis and analysis.

2.2. Hydrogel particle preparation

Hydrogel particles were prepared using a top-down method of mechanical homogenization based on a previously reported methodology (Blomstrand et al., 2022). In brief, 30 % w/w DA-F127 copolymer powder was manually mixed with 70 % w/w water. To induce photopolymerization of the acrylate functional groups, photoinitiator 2-hydroxy-4′-(2-hydroxyethoxy)-2-methylpropiophenone was added to the mixture at a conc. of 0.5 % w/w with respect to the dry DA-F127 weight. The mixture was refrigerated at 4 °C to aid liquification. The cold liquid was then cast into a glass Petri dish and allowed to equilibrate to room temperature (RT) to form a gel. The gel was crosslinked via UV photopolymerization at λ = 302 nm for 3 min, resulting in a bulk hydrogel. The obtained hydrogel was washed in a copious amount of water to remove any non-crosslinked polymer fractions and to facilitate the hydrogel swelling.

The washed hydrogels were ground into particles using a food processor (ErgoMixx, Bosch, Germany), and further homogenized with a disperser, (T18 ULTRA-TURRAX, IKA, Germany) resulting in particle suspension in water. The obtained suspension was suction filtrated using filter paper with a pore size of 6 μm, (Whatman grade 3, Cytiva, Sweden) to remove the excess water, and the obtained filter cake was collected. The wet particle cake post-filtration was divided into two parts: hydrogel particles for further AMP functionalization according to the methodology stated in section 2.2.1 (henceforth referred to as AMP particles), and AMP-free hydrogel particles to act as a control (henceforth referred to as control particles). The prepared particles were stored at −20 °C for short term storage, or, alternatively, freeze-dried for long term storage.

2.2.1. Particle functionalization with the AMP

Freshly filtered particles were functionalized with the AMP using the following procedure. One gram of the wet particle cake post-filtration was dispersed in 5 ml of 0.5 M 2-(N-morpholino) ethanesulfonic acid buffer (MES, pH 6) containing 2 mg/ml of 1-ethyl-3-(3-(dimethylamino)propyl) carbodiimide (EDC) and 2 mg/ml N-hydroxysuccinimide (NHS) and stirred for 30 min. This procedure facilitated the activation of free carboxyl groups in the DA-F127 network via carbodiimide coupling for the subsequent functionalization step with the AMP. Although absent in the native state of Pluronic F127 molecules, free carboxyl group formation in the DA-F127 molecular structure is facilitated by spontaneous hydrolysis of the ester groups present in the polymer structure

after the acrylate group photopolymerization (see **Appendix A, Fig. A.1A**). This phenomenon has been successfully explored for the covalent AMP attachment to DA-F127 hydrogels by previous studies (Atefyekta et al., 2021; Blomstrand et al., 2022). Thereafter, the carboxyl group activation for direct AMP coupling is aided by the EDC and NHS to improve the reaction efficacy and stability of the reactive intermediates (see **Appendix A, Fig. A.1B**).

After the activation step, particle suspension was repeatedly suction filtered by washing with water to remove any activation byproducts. One gram of the activated particles post-filtration was dispersed in 5 ml of 400 µM RRP9W4N AMP in phosphate buffered saline (PBS, pH 7.4) solution and stirred for 2 h to aid direct covalent AMP attachment to the free carboxyl groups via amide bond formation. After the AMP attachment step, particle suspension was repeatedly suction filtered by washing with water to remove any unreacted AMP. The freshly functionalized and suction filtered particles were collected for further analysis.

The filtrate was sampled for the quantification of the AMP uptake into the particles. For this, a UV−Vis spectrophotometer (Multiskan GO, Thermo Fisher Scientific, USA) was used, and absorbance was measured at $\lambda = 280$ nm, which correlates to the absorbance of the tryptophan amino acid end-tag in the AMP structure. The AMP uptake was estimated based on the difference in AMP concentration in the filtrate and the AMP activation solution, using a standard curve.

2.3. Bacterial strains

Staphylococcus aureus CCUG 10778 and methicillin-resistant *Staphylococcus aureus* (MRSA) CCUG 41586 were purchased from the Culture Collection University of Gothenburg (CCUG, Gothenburg, Sweden) and stored long-term at −80 °C after revival. The bacteria were streaked onto brain heart infusion (BHI) agar plates and incubated at 37 °C overnight to obtain single colonies. The agar plates were refrigerated at 4 °C and used within one week.

For each new experiment, a single colony of bacteria was inoculated into 4 ml of tryptic soy broth (TSB) and incubated statically at 37 °C until the mid-log growth stage was reached, determined by optical density measurements at 600 nm (OD_{600}), with an OD_{600} of 0.55–0.75 estimated to correspond to 10^9 colony-forming units per milliliter (CFU/ml). The bacterial suspension was then diluted to the desired target concentration and used for further antibacterial activity assays as described below.

2.4. Antibacterial activity assays individually

2.4.1. Plain AMP and antibiotics

The minimal inhibitory concentration (MIC) of free AMP in liquid (henceforth referred to as plain AMP) as well as the antibiotics VCM and OXA against *S. aureus* and MRSA, were determined using the broth microdilution technique.

MIC of plain AMP was determined in three different culture media conditions i.e., Mueller Hinton broth (MHB), cation-adjusted Mueller Hinton broth (CAMHB), and cation-adjusted Mueller Hinton broth supplemented with 2 % w/v NaCl (CAMHB + NaCl) to determine the effect of salt concentration on AMP activity, and mimic the conditions required for antibiotic testing. In brief, 2-fold serial dilutions of AMP in the chosen culture media (i.e., MHB, CAMHB, or CAMHB + NaCl) were prepared in a 96-well plate, with the final target conc. range of 200–0.2 µM. The bacterial inoculum was prepared from the TSB cultures by diluting the bacteria with the chosen culture media to approximately 10^6 CFU/ml, and finally adding to each well in 1:1 ratio for a final bacteria conc. of $5 * 10^5$ CFU/ml. Well plates were then incubated at 37 °C overnight (∼ 18 h), the OD_{600} read using a UV−vis spectrophotometer with a plate reader and MIC defined as the lowest drug conc. resulting in reduced bacterial growth by more than 80 % compared to an AMP-free growth control.

VCM and OXA MICs were determined in 96-well plates at standard

testing conditions according to the Clinical and Laboratory Standards Institute (CLSI) (Clinical and Laboratory Standards Institute, 2012). CAMHB culture media and overnight incubation (∼ 18 h) at 37 °C or CAMHB + NaCl culture media and incubation at 35 °C for 24 h was used for VCM or OXA susceptibility testing, respectively. After incubation, the antibiotic containing well plates were read at OD_{600} using a plate reader and MIC defined as the lowest drug concentration resulting in more than 80 % reduced bacterial growth compared to antibiotic-free controls.

All antibacterial susceptibility experiments were repeated at least three times, and the MIC values displayed as a concentration interval.

2.4.2. AMP hydrogel particles

The MIC of AMP hydrogel particles was determined by using the broth macrodilution technique in MHB, CAMHB and CAMHB + NaCl culture media against *S. aureus* and MRSA. In brief, 2-fold serial dilutions of freshly functionalized (with 400 µM AMP solution) and suction filtered (>6 µm) AMP hydrogel particles were prepared in a 24-well plate with the final target conc. range of 512–1 mg/ml (swollen particle mass). The bacterial inoculum was prepared from the TSB cultures by diluting the bacteria with the chosen culture media to approximately 10^6 CFU/ml, and then adding it to each well in a 1:1 ratio for a final bacterial conc. of 5×10^5 CFU/ml. A mirror plate of AMP-free hydrogel particles was prepared as the positive control as well as growth control and sterility controls included in each experiment. The plates were placed on a shaker plate under 200 rpm to facilitate component mixing and incubated at 37 °C overnight (∼ 18 h). The following day, MIC values were observed, and MIC defined as the lowest conc. of particles that produced complete inhibition of visible growth.

All antibacterial susceptibility experiments were repeated at least three times, and the MIC values displayed as a concentration interval.

2.5. Checkerboard assays

The combinations of the VCM and OXA antibiotics with (a) plain AMP and (b) AMP hydrogel particles were assessed against *S. aureus* and MRSA using the checkerboard assay technique.

2.5.1. Plain AMP and antibiotics

The effect of the combination of antibiotics and plain AMP was evaluated using the broth microdilution checkerboard assay based on a previously reported method (Bellio et al., 2021). In brief, 2-fold serial dilutions of AMP were prepared along the ordinate of a 96-well plate in sub-MIC conc., with varying final conc. (50–0.39 µM). Following this, a crosswise 2-fold dilution of the antibiotic was prepared along the abscissa (see **Appendix A, Fig. A.2A** for graphical representation). The final conc. depended on the chosen antibiotic type, with VCM tested in conc. range of 32–0.03 µg/ml and OXA in a conc. range of 64–0.06 µg/ml. The cell media type was chosen based on the CLSI guidelines i.e., all VCM checkerboard assays were conducted in CAMHB, while all OXA assays were performed in CAMHB + NaCl. The bacterial inoculum was prepared from the TSB cultures by diluting the bacteria with the chosen cell culture media to approximately 10^6 CFU/ml and then added to all wells of the 96-well plate in a 1:1 ratio for a final bacterial concentration of 5×10^5 CFU/ml. For each organism and AMP-antibiotic combination, additional dilution series for the AMP and antibiotic as well as a growth control not containing any AMP or antibiotics, were included. The plates were incubated at 37 °C overnight (∼18 h) for VCM and at 35 °C for 24 h for OXA. The following day, OD_{600} was read using a plate reader, and MIC was defined as the lowest drug conc. resulting in more than 80 % reduction in bacterial growth compared to the growth control.

The interaction type between the AMP and antibiotics was determined using the fractional inhibitory concentration (FIC) index. The FIC index was calculated for each AMP-antibiotic concentration combination from the observed MIC values of AMP and antibiotics using the following equations:

$$FIC_{AMP} = \frac{MIC_{AMP} \; in \; combination}{MIC_{AMP} \; alone} \qquad (1)$$

$$FIC_{Antibiotic} = \frac{MIC_{Antibiotic} \; in \; combination}{MIC_{Antibiotic} \; alone} \qquad (2)$$

$$FIC = FIC_{AMP} + FIC_{Antibiotic} \qquad (3)$$

The calculated FIC index values were averaged along the turbidity/non-turbidity interface of each well-plate. Ultimately, the mean FIC index was averaged over an experimental triplicate, and the determined FIC value was used to categorize results, where an FIC index $\leq$ 0.5 was interpreted as synergistic, $0.5 <$ FIC ≤ 1.0 as additive, $1.0 <$ FIC ≤ 4.0 as indifferent, and FIC > 4.0 as antagonistic interactions between the AMP and antibiotic (Zhu et al., 2021; Mataraci and Dosler, 2012; Bonapace et al., 2000).

2.5.2. AMP hydrogel particles and antibiotics

The effect of the OXA antibiotic and AMP hydrogel particle combination was evaluated using a modified broth macrodilution checkerboard assay. Freshly functionalized (with 400 µM AMP solution) and suction filtrated AMP particles were used to prepare a particle suspension in CAMHB at four times the desired highest particle suspension conc. (e.g., 32 x 4 = 128 mg/ml for 32 mg/ml). Two-fold serial dilutions of AMP particles were prepared along the abscissa of a 24-well plate in sub-MIC conc. with varying final conc. (32–1 mg/ml in swollen particle mass). Following this, OXA solutions in CAMHB were prepared by diluting the OXA stock solution (3 mg/ml in H_2O). Four separate vials with four times the desired final OXA conc. (e.g., 32 x 4 = 128 µg/ml for 32 µg/ml) were prepared. OXA solution was then added to the AMP particles in the 24-well plate at 1:1 ratio, with each row containing one conc., with final conc. series of 32, 16, 8 and 4 µg/ml, respectively, simulating a 2-fold dilution series along the ordinate (see Appendix A, Fig. A.2B for graphical representation). The MRSA inoculum was prepared from the TSB cultures by diluting the bacteria with the CAMHB to approximately 10^6 CFU/ml and then added to all wells of the 24-well plate in 1:1 ratio for a final bacteria conc. of 5 * 10^5 CFU/ml. A mirror plate of AMP-free hydrogel particles as a positive control was prepared as well as growth and sterility control wells included in each experiment. The prepared plates were placed on a shaker plate at 200 rpm to facilitate the component mixing and incubated at 35 °C for 3 h. After 3 h the plates were removed from the incubator and 67 µl of aqueous NaCl solution (32 % w/v) was added to every 1 ml test solution to generate 2 % w/v of final NaCl conc. in every well. A delayed salt addition methodology was devised to limit the AMP inactivation due to high sodium ion content and resulting loss of antibacterial activity. Ultimately, the plates were returned to the incubator and incubated under shaking at 35 °C for 24 h. MIC values were observed the following day with MIC defined as the lowest conc. of particle-OXA combination that produced complete inhibition of visible growth. The resulting FIC index was calculated along the observable growth/no growth interface according to the methodology stated in section 2.5.1.

2.6. Scanning electron microscopy (SEM)

SEM (Leo Ultra 55, Carl Zeiss, Germany) was utilized at a 2 kV accelerating voltage to investigate the particle interaction with bacteria and observe any changes in bacterial morphology. For this, AMP particles and AMP-free control particles were placed in a 24-well plate and inoculated with a high inoculum MRSA at 10^8 CFU/ml in 10 % v/v TSB followed by overnight incubation at 37 °C. The following day, the particles were carefully washed in PBS, followed by fixation and dehydration procedure. The particles were immersed in 4 % formaldehyde solution (VWR, Sweden) for 2 h, followed by successive 15 min dehydration steps in an ethanol solution gradient (20 %, 50 %, 70 %, 85 %, and 99.9 % v/v). Finally, the particles were immersed in 50 % v/v

hexamethyldisilazane (HDMS) solution in ethanol for 30 min, followed by 100 % HDMS. The HDMS was allowed to fully evaporate overnight under a fume hood. The dried particles were then mounted onto SEM sample holders and coated with 5 nm layer of gold using a sputter coater (EM ACE600, Leica Microsystems) prior to SEM imaging.

2.7. Optical microscopy

An optical microscope was utilized to image the rehydrated particles and analyze their morphology in the swollen state. For this a stereo microscope (Stemi 508, Carl Zeiss AG, Germany) equipped with a digital camera was used and the hydrogel particles were rehydrated in Milli-Q water prior to imaging.

2.8. Drug delivery from the control hydrogel particles

To investigate the potential of using hydrogel particles as drug delivery systems for localized delivery of antibiotics, OXA and VCM were used as model drugs. Further experimental details of particle loading and drug delivery experiments are presented in Appendix A (**Supporting Text 1**).

3. Results and discussion

3.1. AMP-functionalized hydrogel particles

The covalently functionalized AMP hydrogel particles investigated in the present study were formed according to the procedure developed by E. Blomstrand *et al.* (Blomstrand et al., 2022). Similar to the previously described method, the hydrogel particles were manufactured from crosslinked lyotropic liquid crystal hydrogels made from diacrylate Pluronic F127 (DA-F127) block copolymers via a top-down technique. An SEM micrograph of the final freeze-dried particles can be seen in Fig. 1**B**, with the dried particles appearing as a powder, as shown in Fig. 1**C**. The prepared particles had a distinctly asymmetrical geometry and irregular profiles due to the top-down manufacturing method of mechanical homogenization.

The covalent immobilization of RRP9W4N AMP was achieved via carbodiimide chemistry, resulting in direct AMP coupling to the hydrogel particle network via amide bond formation. The successful AMP integration was confirmed through UV−Vis spectroscopy, revealing an approximate 3 % w/w AMP uptake within the dry particle structure, which is in line with the previously reported values (Blomstrand et al., 2022). These findings correlate directly with previous studies on the AMP particles, where AMP covalent immobilization has been demonstrated by various spectroscopy techniques (UV–Vis, FT-IR, Raman and XPS) as well as leaching studies and zone of inhibition experiments, with no detectable AMP leaching reported (Blomstrand et al., 2022; Stepulane et al., 2022; Atefyekta et al., 2021).

Regarding the size distribution of the AMP particles as well as the AMP-free control particles, previous dynamic light scattering (DLS) studies on the particle suspensions have concluded that 99.8 % w/w of the particle mass is distributed between 100 µm and 500 µm, with maximum number-based distribution between 2 µm and 30 µm (Blomstrand et al., 2022). Both particle types utilized in the current study were filtered through a 6 µm pore size filter paper during processing, removing the lower fractions of the number-based distribution, as seen in the microscopy images of rehydrated and dried particles in Fig. 1**A and B**, respectively. However, since DLS assumes a spherical particle geometry, it is worth noting that some error is to be expected in the estimation of the particle size distribution.

Most importantly, the AMP particles utilized in the present study have previously demonstrated high antibacterial efficacy against *S. aureus, S. epidermidis, E. coli,* two different MRSA strains as well as *P. aeruginosa* to a lesser extent, with MIC values of 26–103, 26–52, 52–103, 13–52 and 413–825 µg/ml (0.8–3.1, 0.8–1.6, 1.6–3.1, 0.4–1.6
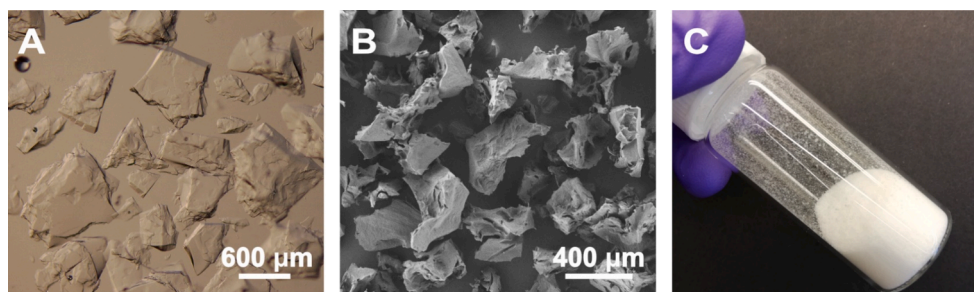
Fig. 1. Stereo microscopy image of the rehydrated AMP hydrogel particles (A), SEM micrograph of the freeze-dried control particles (B), photograph of the freeze-dried control particle powder (C).

and 12.5–25 mg/ml in dry particle mass), respectively, corroborating the broad-spectrum contact-killing potential of the immobilized AMP. Furthermore, the AMP particles have also been shown to display no cytotoxic or hemolytic effect, along with improved stability against serum, where a high antibacterial effect against *S. epidermidis* has been retained for 2 days, compared to plain AMP losing all of its antibacterial potency within a day (Blomstrand et al., 2022).

3.2. Antibacterial activity of the antibacterial agents individually

The antibacterial activity of all individual antibacterial agents utilized in the study, namely the antibiotics VCM and OXA as well as plain AMP and AMP particles, was tested against *S. aureus* and MRSA, with the results presented in Table 1.

Three different cell culture media types were employed, namely, MHB, CAMHB and CAMHB + NaCl. Different media types were utilized to comply with the standard testing conditions for VCM and OXA according to the CLSI antibacterial susceptibility test methodology (Clinical and Laboratory Standards Institute, 2012). In order to produce reliable MIC values, several requirements must be fulfilled for certain antibiotics and antibiotic/species combinations; namely, additional supplementation of MHB with Ca^{2+} and Mg^{2+} ions is necessary for accurate detection of VCM resistance in staphylococci, and addition of 2 % w/v NaCl to CAMHB is required for testing of OXA resistance in order to improve the detection of heteroresistant MRSA. As expected, VCM activity was high for both *S. aureus* and MRSA with MICs of 0.5–1 μg/ml and 1–2 μg/ml, respectively, consistent with the susceptibility

breakpoint of 2 μg/ml (Tenover and Moellering, 2007; Baltch et al., 2007). Similarly, in accordance with the expected susceptibility and resistance to OXA, MICs of 0.06–0.25 μg/ml were observed for regular *S. aureus* and 16–32 μg/ml for MRSA (Baltch et al., 2007).

As evident from Table 1, the variation in media type significantly impacted the antibacterial activity of plain AMP and the resulting MIC values for both *S. aureus* and MRSA. For *S. aureus*, plain AMP exhibited comparable MIC values between 12–24 μg/ml in both MHB and CAMHB, with a substantial 4- to 8-fold increase to 96 μg/ml in CAMHB+NaCl. A similar trend was observed for the MRSA, with AMP displaying increasing MIC values of 6–12, 12–24 and 48–96 μg/ml in MHB, CAMHB and CAMHB + NaCl, respectively. Given that CAMHB and CAMHB + NaCl have higher cation concentrations compared to MHB, the bacterial susceptibility to AMP is expected to decrease. This is because the presence of Na^+, Ca^{2+}, and Mg^{2+} ions is known to cause substantial inhibition of cationic AMPs (Wiegand et al., 2008). Indeed, high salt concentration is one of the key challenges in therapeutic applications of soluble AMPs, where the salt-induced shielding of the cationic charge can lead to peptide inactivation (Lim et al., 2013). The covalent attachment of AMP has been proposed as a potential solution, further motivating the development of AMP hydrogel particles (Onaizi and Leong, 2011; Li et al., 2014).

Upon covalently attaching the AMPs onto the hydrogel particles, a MIC value of 0.8–1.6 mg/ml and 3.2 mg/ml (dry particle mass) was observed for *S. aureus* in MHB and CAMHB, respectively. No MIC could be detected in CAMHB + NaCl, as bacterial growth was observed at the highest AMP particle test concentration, where the particles no longer behaved like a dispersion, but exhibited a slurry-like consistency. When the obtained MIC values were adjusted to the corresponding AMP uptake in μg/ml from the UV–Vis data, a MIC equivalent to 26 –52 μg/ml and 104 μg/ml was observed in MHB and CAMHB, respectively, corresponding to 2- and 5-fold increase when compared to plain AMP. These results are anticipated, as AMP covalent attachment is generally associated with loss of antibacterial activity, contributing to the reduced AMP particle MICs against *S. aureus*.

Overall, it is important to emphasize that, due to the hydrogel particles' ability to swell and take up aqueous solutions, it is highly likely that only a fraction of the covalently attached AMP is located on the particle surface, with some portion being bound within the particle bulk. Since AMPs require direct contact to exert their contact-killing antibacterial mechanism, this could result in only a fraction of the attached AMP being active and able to contribute to the observed antibacterial effect, potentially leading to an underestimation of the obtained AMP particle MIC values, with the possibility of even lower actual MICs. For these reasons, AMP particle MIC values are presented in the original mg/ml values as definitive MIC value as well as the μg/ml derived from the UV–Vis AMP uptake data.

Furthermore, the AMP particles displayed equally high activity against MRSA compared to *S. aureus* – an observation consistent with previous work performed by Blomstrand *et al.* – with identical MIC values detected in MHB and CAMHB (Blomstrand et al., 2022). This

Table 1
Antibacterial activity of the individually tested agents against *S. aureus* and MRSA in different cell culture media.

	MIC (μg/ml)		
	Culture media		
	MHB	CAMHB	CAMHB + NaCl
***S. aureus,* CCUG 10778**			
AMP	12–24	12–24	96
Vancomycin	–	0.5–1[a]	–
Oxacillin	–	–	0.06–0.25[a]
AMP particles	26–52[b]	104[b]	–[d]
	(0.8–1.6 mg/ml)[c]	(3.2 mg/ml)[c]	
MRSA, CCUG 41586			
AMP	6–12	12–24	48–96
Vancomycin	–	1–2[a]	–
Oxacillin	–	–	16–32[a]
AMP particles	26–52[b]	104[b]	–[d]
	(0.8–1.6 mg/ml)[c]	(3.2 mg/ml)[c]	

[a] at standard testing conditions according to the CLSI methodology (Clinical and Laboratory Standards Institute, 2012).
[b] calculated AMP concentration in the AMP particles, μg/ml.
[c] AMP particle concentration in dry mass, mg/ml.
[d] MIC not observed at the highest AMP particle test concentration of 832 μg/ml (25.6 mg/ml in dry mass).

result directly indicates the AMP's membrane-targeting MOA, due to the electrostatic attraction between the cationic arginine in the AMP structure and the negatively charged peptidoglycan layer of the Gram-positive bacteria cell envelope. This interaction leads to broad-spectrum antibacterial activity, regardless of the bacteria's resistance profile to conventional antibiotics. To further illustrate this, AMP particles were inoculated with a high inoculum of MRSA (10^8 CFU/ml) and incubated overnight, followed by bacterial fixation and SEM imaging. As evident from Fig. 2, drastic changes in the bacterial cell morphology as well as growth patterns could be observed. Generally, a denser cell coverage was observed on the control particles, with a large population of bacteria present. With no significant observable changes in the cell morphology, bacteria appeared to form multilayered structures reminiscent of microcolony formation in early-stage biofilm development. In contrast, MRSA displayed a scattered growth pattern on the AMP particles, with fewer cells and no evidence of cell division or microcolony formation. Notably, a drastic change in the cell morphology could be observed with the individual MRSA cells exhibiting strong adherence to the hydrogel substrate, resulting in damaged cell envelopes and loss of overall integrity. It is worth noting that small, round particle-like features at a length scale smaller than the bacteria were seen on the AMP particle surface, most likely stemming from the cell media component precipitation and deposition, caused by the strong electrostatic effect of the AMP – an issue commonly observed with cationic AMPs. Overall, these observations serve as visual evidence of the strong antibacterial effect AMP hydrogel particles exert on the bacterial cells.

3.3. Plain AMP interaction with antibiotics

The antibacterial activity of the plain AMP in combination with VCM and OXA antibiotics was studied against *S. aureus* and MRSA using the checkerboard assays, with the results presented in Table 2, where an FIC index ≤ 0.5 was interpreted as synergistic, $0.5 < \text{FIC} \leq 1.0$ as additive, $1.0 < \text{FIC} \leq 4.0$ as indifferent, and FIC > 4.0 as antagonistic interaction.

Table 2
Antibacterial activity of the plain AMP in combination with antibiotics against *S. aureus* and MRSA as determined by the checkerboard assay.

Agent combination	MIC (µg/ml)		Minimum FIC index[b]	Mean FIC index[c]	Interaction type
	Alone	Combined[a]			
***S. aureus*, CCUG 10778**					
AMP	24.13	12.06	0.53	0.94	additive
Vancomycin	1.00	0.03			
AMP	96.50	3.02	0.53	0.75	additive
Oxacillin	0.25	0.13			
MRSA, CCUG 41586					
AMP	24.13	6.03	0.53	0.87	additive
Vancomycin	2.00	0.06			
AMP	96.50	12.06	0.25	0.39	synergistic
Oxacillin	32.00	0.06			

[a] MIC at minimum FIC index.
[b] minimum FIC index corresponds to the agent conc. combination with lowest possible FIC index and no observable growth.
[c] mean FIC index corresponds to an average of all FICs along the observable growth/no growth interphase.

In general, plain AMP displayed additive or synergistic interactions with both VCM and OXA to varying degrees, depending on the bacterial strain. No antagonism was observed with any AMP-antibiotic combination. On average, the AMP-VCM combination exhibited lower antibacterial interaction potential than AMP-OXA, most likely due to the already high initial antibacterial activity of VCM.

With AMP-VCM combination, a mean FIC index of 0.94 and 0.87 was obtained against *S. aureus* and MRSA, respectively, implying an overall additive interaction between the two agents, with slightly increased potential toward MRSA. Notably, a 33-fold reduction in VCM MIC (from 1 µg/ml to 0.03 µg/ml for *S. aureus,* from 2 µg/ml to 0.06 µg/ml for MRSA) was more pronounced than the mere 2-fold reduction in AMP MIC (from 24.13 µg/ml to 12.06 µg/ml for *S. aureus*, from 24.13 µg/ml
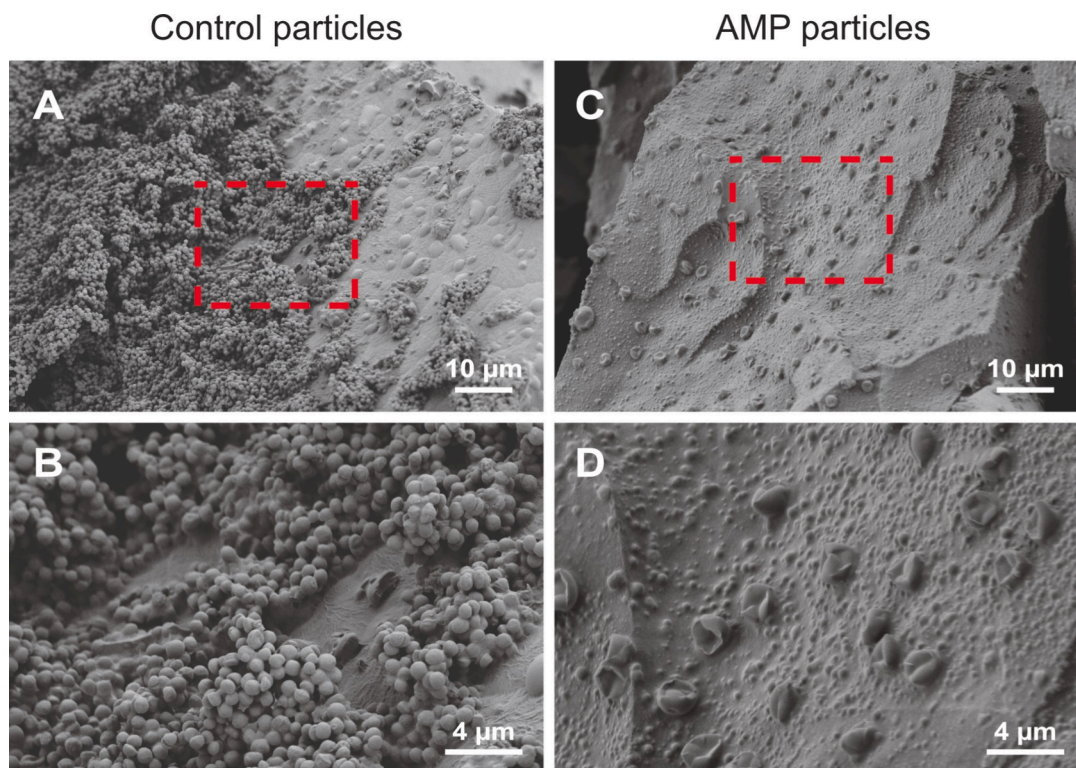

Control particles   AMP particles

Fig. 2. SEM micrographs of AMP-free control particles (A, B) and AMP particles (C, D) after overnight incubation with high inoculum of MRSA. The presence of AMP notably influenced the bacterial cell count, morphology, and growth pattern.

to 6.03 μg/ml for MRSA) at the minimum FIC of 0.53 for both *S. aureus* and MRSA. The most likely explanation for the lower activity of the AMP stems from the peptide inactivation in the presence of CAMHB, as discussed previously.

For AMP-OXA combination, a mean FIC index of 0.75 was obtained against *S. aureus* consistent with an additive antibacterial effect. In contrast to the AMP-VCM combination, OXA showed only 2-fold reduction in MIC (from 0.25 μg/ml to 0.13 μg/ml) in comparison to stark 32-fold reduction of AMP MIC (from 96.50 μg/ml to 3.02 μg/ml) at the minimum FIC index of 0.53. Significantly, upon combining AMP and OXA against MRSA, a notably increased antibacterial activity could be observed with a mean FIC index of 0.39, down to the minimum FIC index of 0.25, displaying strong antibacterial synergism between the two compounds. Notably, OXA showed 512-fold reduction in MIC (from 32 μg/ml to 0.06 μg/ml), whilst AMP experienced a more moderate 8-fold reduction in MIC (from 96.50 μg/ml to 12.06 μg/ml) at the minimum FIC index against MRSA.

Despite the test media limitations on the AMP-antibiotic combinations, the *in vitro* results of the plain AMP interactions showed promise, especially between plain AMP and OXA against MRSA, warranting further investigation of the AMP-functionalized hydrogel particle combination with OXA.

3.4. AMP particle interaction with oxacillin antibiotic against MRSA

To investigate the interaction potential between OXA antibiotic and AMP hydrogel particles against MRSA, a modified checkerboard assay was utilized. As previously discussed in section 3.2, the change in cell culture media has a stark effect on the antibacterial activity of both the plain AMP and AMP particles separately, with no MIC detected for AMP particles in CAMHB + NaCl. Therefore, to circumvent the AMP particle inactivation by the high Na^+ ion concentration and the related issues in the OXA checkerboard testing, a late NaCl addition method was devised. More specifically, a 3 h delay was introduced for the NaCl addition to the test cultures to hinder AMP particle inactivation. Killing kinetics of AMPs are generally considered to be rapid due to the electrostatic attraction between the peptides and negatively charged components in the bacterial cell envelopes, ranging from seconds to minutes (Lim and Leong, 2018). Therefore it was theorized that 3 h would be an optimal timepoint to allow AMP particles to interact with the MRSA, while not diminishing reliable determination of OXA MIC. Since the delayed NaCl addition does not directly affect the mechanism of action of OXA, it was deemed suitable for AMP particle synergy testing while maintaining reliable accuracy.

The obtained results from the OXA-AMP particle checkerboard assays against MRSA can be seen in Table 3, displayed as the determined FIC indexes and the observable growth/no growth gradient at different OXA-AMP particle combinations, where shaded area in yellow represent the wells with observable bacterial growth. In general, the OXA-AMP particle combination displayed positive synergistic effect with significant enhancement of the antibacterial activity of both compounds in sub-MIC concentrations. Markedly, a maximum of 64-fold reduction in OXA MIC (from 32 μg/ml to 0.5 μg/ml) was observed in combination with the AMP particles. Similarly, a reduction in the AMP particle MIC was observed, with a maximum of 32-fold reduction from 104 μg/ml to 3.25 μg/ml (from 3.2 mg/ml to 0.1 mg/ml in dry particle mass) upon combination with OXA. Overall OXA and AMP particle interaction can be considered as synergistic, resulting in a mean FIC index of 0.22 (Bonapace et al., 2002).

Ultimately, from the conducted checkerboard tests it was concluded that the OXA antibiotic can react synergistically in combination with both plain AMP and AMP-functionalized hydrogel particles, displaying enhanced antibacterial effects against MRSA. However, it is worth noting that, upon covalent immobilization of the AMP onto the hydrogel particles, a consecutive decrease in the synergism with OXA was observed, from 512-fold MIC reduction to 64-fold MIC reduction with plain AMP and AMP particles, respectively, when compared to OXA alone (see Fig. 3). This observation can be directly linked to the reduction in peptide availability and accessibility upon immobilization, reported previously both for the RRP9W4N investigated in the present study as well as multiple other types of AMPs (Blomstrand et al., 2022; Costa et al., 2011). Despite the commonly observed reduction in antibacterial efficacy prevalent in chemically tethered AMPs, our study demonstrated that AMP covalent attachment to hydrogel particles maintained high synergism with OXA, even at reduced antibacterial activity.

As to the potential synergism mechanisms between the plain AMP and the AMP hydrogel particles with OXA, further insights are needed into the MOA of both RRP9W4N alone, and upon covalent immobilization, to draw more concrete conclusions.

OXA is a narrow-spectrum Gram-positive β-lactam antibiotic that works by inhibiting the cell wall biosynthesis process. Generally, β-Lactams inhibit the synthesis of the peptidoglycan layer in the bacterial cell wall by binding to the penicillin binding proteins (PBPs), thereby halting the crosslinking phase of the cell wall synthesis. MRSA has evolved resistance to all β-lactams, including OXA, conferred by the *mecA* gene – a gene encoding for an altered penicillin binding protein (PBP2a) with low affinity for β-lactams (Peacock and Paterson, 2015).

With OXA resistance mechanisms in MRSA well understood, literature on OXA-AMP or other AMP-like antibacterial agent combinations

Table 3

FIC indexes for the AMP particle and oxacillin combination against MRSA. Shaded areas in yellow respective of the wells with observable bacterial growth. Mean FIC index determined along the observable growth/no growth interface shaded in grey.

		AMP particles, μg/ml					
		104 [a]	**52**	**26**	**13**	**6.5**	**3.25**
	32 [a]	2.00	1.50	1.25	1.13	1.06	1.03
	16	1.50	1.00	0.75	0.63	0.56	0.53
Oxacillin, μg/mg	**8**	1.25	0.75	0.50	0.38	0.31	0.28
	4	1.13	0.63	0.38	0.25	0.19	0.16
	2	1.06	0.56	0.31	0.19	0.13	0.09
	1	1.03	0.53	0.28	0.16	0.09	0.06
	0.5	1.02	0.52	0.27	0.14	0.08	0.05

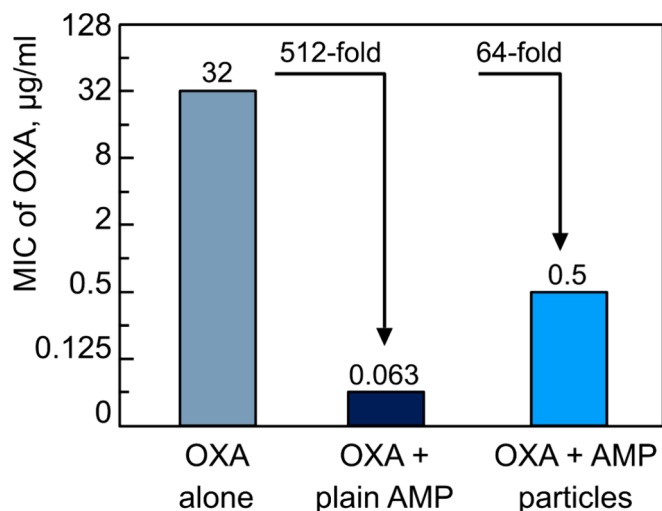[a]MIC of OXA and AMP particles alone at CAMHB.

Fig. 3. Antibacterial activity of oxacillin alone and in combination with plain AMP or AMP hydrogel particles against MRSA. A decrease in synergism compared to plain AMP was observed upon covalent immobilization of AMP onto the hydrogel particles.

does not yield any universal mechanistic conclusions on the possible MOA of such combinations. This is expected, as AMP interaction mechanisms with the bacterial cell envelope, despite common structural features and functionality, can vary significantly and are highly dependent on the specific peptide structure.

Previous studies on antibiotic-AMP combinations have suggested that synergism mainly occurs between highly membrane-active AMPs and antibiotics with intracellular targets like OXA (Zharkova et al., 2019). For example, MDR *E. coli* have been reported to exhibit increased susceptibility to AMP, partly through regulatory changes shaping the lipopolysaccharide composition of the bacterial outer membrane (Lázár et al., 2018). More specifically, a synthetic antibacterial peptide conjugate ASU014 composed of a *S. aureus* binding and an inhibitory peptide has been previously shown to exhibit synergy with OXA against MRSA both *in vitro* and in a MRSA skin infection model, with no insights on the possible MOA (Lainson et al., 2017).

RRP9W4N, the AMP investigated in this study, is a relatively short AMP consisting of only 13 amino acids. With *S. aureus* cell wall thickness estimated to range between 20–40 nm, and thickening upon methicillin resistance acquisition, it is plausible to assume that plain RRP9W4N is unable to translocate the cell envelopes (Lim et al., 2015; García et al., 2017). Furthermore, upon covalent immobilization of RRP9W4N, a further reduction in the AMP's degree of freedom is expected. It is therefore unlikely for the AMP particles to breach the bacterial membranes and form transient pores. Based on the AMP particle antibacterial activity alone, it can therefore be speculated that AMP particles interact with MRSA by increasing the bioavailability of OXA, similar to membrane permeabilizers, resulting in the observed OXA-AMP particle synergism.

Alternatively, MRSA resistance itself could lead to a reduction in plasma membrane charge, as demonstrated previously with daptomycin antibiotic and OXA synergistic combinations, facilitating the OXA-AMP interactions observed in this study. Daptomycin is one of only three clinically approved membrane-targeting AMPs, potentially providing some insight into how membrane-active peptides could synergize with antibiotics (Huang, 2020). Some previous studies have concluded that β-lactam antibiotics enhance the daptomycin binding to MRSA by reducing the charge of the plasma membrane (Molina and Huang, 2016). Some authors have hypotheses that insertion of daptomycin into the cell membrane can alter peptidoglycan precursors, leading to PBP2a being unable to perform its crosslinking function in the presence of OXA. Additionally, some studies have suggested that daptomycin could affect

the levels or functionality of one or more factors required for the full expression of the resistance gene *mecA* in MRSA in the presence of OXA (Rand and Houck, 2004).

Overall, based on the conclusion of similar antibiotic-AMP systems, it is possible to only speculate on the unelucidated factors that determine the synergistic effect between the plain AMP and the AMP particles with OXA observed in this study.

The findings of this study demonstrate how the well-known AMP-antibiotic synergism can be effectively translated to AMP-functionalized biomaterial surfaces, highlighting their potential applicability in conjunction with conventional antibiotics for combating drug resistant infections. With major significance in medical devices and wound care, AMP-functionalized hydrogel particles have application potential in combination with systemic antibiotic therapy or as antibiotic delivery system. DA-F127 hydrogels, known for their high water content, have been previously explored in drug delivery systems (Veyries et al., 1999). As a proof-of-concept, we investigated the VCM and OXA delivery from the AMP-free control particles (see **Appendix A**, **Fig. A1**). The control particles were able to load both VCM and OXA, however exhibiting rapid release without sustained delivery profile. Therefore, further modification is needed to fully harness the synergistic potential of AMP-functionalized hydrogel particles with antibiotics for a multifunctional material platform.

4. Conclusions

This study investigates the combined antibacterial efficacy and potential synergism of plain RRP9W4N antimicrobial peptide (AMP) and AMP-functionalized hydrogel particles together with conventional antibiotics – vancomycin (VCM) and oxacillin (OXA). Checkerboard assays revealed additive and synergistic interactions between the plain AMP-VCM and plain AMP-OXA combinations against *S. aureus* and MRSA, with OXA showing particularly high synergism. Notably, the AMP-OXA combination displayed a significant synergistic effect against MRSA, with a 512-fold reduction in OXA MIC values when combined with plain AMP. The observed synergism with OXA against MRSA was retained upon covalent AMP immobilization onto the hydrogel particles, albeit at a lower rate, with a 64-fold reduction in OXA MIC, indicating a potential trade-off between the AMP stability and antibacterial efficacy. In the context of medical devices, these findings emphasize the potential of AMP-functionalized biomaterial surfaces to provide combined antibacterial effects alongside antibiotics, offering a promising strategy for fighting drug resistant biomaterial-associated infections and reversal of antimicrobial resistance.

CRediT authorship contribution statement

Annija Stepulane: Writing – original draft, Visualization, Methodology, Investigation, Conceptualization. **Anand Kumar Rajasekharan:** Writing – review & editing, Supervision. **Martin Andersson:** Writing – review & editing, Supervision, Funding acquisition, Conceptualization.

Declaration of competing interest

The authors declare the following financial interests/personal relationships which may be considered as potential competing interests: Annija Stepulane reports equipment, drugs, or supplies and writing assistance were provided by Amferia AB. Martin Andersson reports a relationship with Amferia AB that includes: board membership. Anand Kumar Rajasekharan reports a relationship with Amferia AB that includes: employment. Annija Stepulane reports a relationship with Amferia AB that includes: employment. If there are other authors, they declare that they have no known competing financial interests or personal relationships that could have appeared to influence the work reported in this paper.

Data availability

Data will be made available on request.

Acknowledgments

Appendix A. Supplementary data

Reaction scheme of the Pluronic DA-F127 polymerization and functionalization with antimicrobial peptides, graphical illustration of the checkerboard assay methodology used in the synergy testing, and vancomycin and oxacillin antibiotic delivery methodology and release curves from the control hydrogel particles. Supplementary data to this article can be found online at https://doi.org/10.1016/j.ijpharm.2024.124630.

References

Almaaytah, A., Abualhaijaa, A., Alqudah, O., 2019. The evaluation of the synergistic antimicrobial and antibiofilm activity of AamAP1-Lysine with conventional antibiotics against representative resistant strains of both Gram-positive and Gram-negative bacteria. Infect. Drug Resist. 12, 1371–1380. https://doi.org/10.2147/IDR.S204626.

Atefyekta, S., Blomstrand, E., Rajasekharan, A.K., Svensson, S., Trobos, M., Hong, J., Webster, T.J., Thomsen, P., Andersson, M., 2021. Antimicrobial peptide-functionalized mesoporous hydrogels. ACS Biomater. Sci. Eng. 7, 1693–1702. https://doi.org/10.1021/acsbiomaterials.1c00029.

Bahar, A., Ren, D., 2013. Antimicrobial Peptides. Pharmaceuticals 6, 1543–1575. https://doi.org/10.3390/ph6121543.

Baltch, A.L., Ritz, W.J., Bopp, L.H., Michelsen, P.B., Smith, R.P., 2007. Antimicrobial activities of daptomycin, vancomycin, and oxacillin in human monocytes and of daptomycin in combination with gentamicin and/or rifampin in human monocytes and in broth against Staphylococcus aureus. Antimicrob. Agents Chemother. 51, 1559–1562. https://doi.org/10.1128/AAC.00973-06.

Bellio, P., Fagnani, L., Nazzicone, L., Celenza, G., 2021. New and simplified method for drug combination studies by checkerboard assay. MethodsX 8. https://doi.org/10.1016/j.mex.2021.101543.

Blomstrand, E., Rajasekharan, A.K., Atefyekta, S., Andersson, M., 2022. Cross-linked lyotropic liquid crystal particles functionalized with antimicrobial peptides. Int. J. Pharm. 627, 122215 https://doi.org/10.1016/j.ijpharm.2022.122215.

Blomstrand, E., Atefyekta, S., Rajasekharan, A.K., Andersson, M., 2023. Clinical investigation of use of an antimicrobial peptide hydrogel wound dressing on intact skin. J. Wound Care 32, 368–375. https://doi.org/10.12968/jowc.2023.32.6.368.

Bonapace, C.R., White, R.L., Friedrich, L.V., Bosso, J.A., 2000. Evaluation of antibiotic synergy against Acinetobacter baumannii: a comparison with Etest, time-kill, and checkerboard methods. Diagn. Microbiol. Infect. Dis. 38, 43–50. https://doi.org/10.1016/S0732-8893(00)00163-2.

Bonapace, C.R., Bosso, J.A., Friedrich, L.V., White, R.L., 2002. Comparison of methods of interpretation of checkerboard synergy testing. Diagn. Microbiol. Infect. Dis. 44, 363–366. https://doi.org/10.1016/S0732-8893(02)00473-X.

Cesaro, A., Lin, S., Pardi, N., de la Fuente-Nunez, C., 2023. Advanced delivery systems for peptide antibiotics. Adv. Drug Deliv. Rev. 196, 114733 https://doi.org/10.1016/j.addr.2023.114733.

Cleophas, R.T.C., Sjollema, J., Busscher, H.J., Kruijtzer, J.A.W., Liskamp, R.M.J., 2014. Characterization and activity of an immobilized antimicrobial peptide containing bactericidal PEG-hydrogel. Biomacromolecules 15, 3390–3395. https://doi.org/10.1021/bm500899r.

Clinical and Laboratory Standards Institute, 2012. Methods for Dilution Antimicrobial Susceptibility Tests for Bacteria That Grow Aerobically; Approved Standard — Ninth Edition.

Costa, F., Carvalho, I.F., Montelaro, R.C., Gomes, P., Martins, M.C.L., 2011. Covalent immobilization of antimicrobial peptides (AMPs) onto biomaterial surfaces. Acta Biomater. 7, 1431–1440. https://doi.org/10.1016/j.actbio.2010.11.005.

García, A.B., Viñuela-Prieto, J.M., López-González, L., Candel, F.J., 2017. Correlation between resistance mechanisms in Staphylococcus aureus and cell wall and septum thickening. Infect. Drug Resist. 10, 353–356. https://doi.org/10.2147/IDR.S146748.

Grassi, L., Maisetta, G., Esin, S., Batoni, G., 2017. Combination strategies to enhance the efficacy of antimicrobial peptides against bacterial biofilms. Front. Microbiol. 8, 314440 https://doi.org/10.3389/fmicb.2017.02409.

Haque, M., Sartelli, M., McKimm, J., Abu Bakar, M.B., 2018. Health care-associated infections – an overview. Infect. Drug Resist. 11, 2321–2333. https://doi.org/10.2147/IDR.S177247.

Huang, H.W., 2020. DAPTOMYCIN, its membrane-active mechanism vs. that of other antimicrobial peptides. Biochim. Biophys. Acta - Biomembr. 1862, 183395 https://doi.org/10.1016/j.bbamem.2020.183395.

Kazemzadeh-Narbat, M., Cheng, H., Chabok, R., Alvarez, M.M., de la Fuente-Nunez, C., Phillips, K.S., Khademhosseini, A., 2021. Strategies for antimicrobial peptide coatings on medical devices: a review and regulatory science perspective. Crit. Rev. Biotechnol. 41, 94–120. https://doi.org/10.1080/07388551.2020.1828810.

Lainson, J.C., Daly, S.M., Triplett, K., Johnston, S.A., Hall, P.R., Diehnelt, C.W., 2017. Synthetic antibacterial peptide exhibits synergy with oxacillin against MRSA. ACS Med. Chem. Lett. 8, 853–857. https://doi.org/10.1021/acsmedchemlett.7b00200.

Lázár, V., Martins, A., Spohn, R., Daruka, L., Grézal, G., Fekete, G., Számel, M., Jangir, P. K., Kintses, B., Csörgő, B., Nyerges, Á., Györkei, Á., Kincses, A., Dér, A., Walter, F.R., Deli, M.A., Urbán, E., Hegedűs, Z., Olajos, G., Méhi, O., Bálint, B., Nagy, I., Martinek, T.A., Papp, B., Pál, C., 2018. Antibiotic-resistant bacteria show widespread collateral sensitivity to antimicrobial peptides. Nat. Microbiol. 3, 718–731. https://doi.org/10.1038/s41564-018-0164-0.

Lewies, A., Wentzel, J.F., Jordaan, A., Bezuidenhout, C., Du Plessis, L.H., 2017. Interactions of the antimicrobial peptide nisin Z with conventional antibiotics and the use of nanostructured lipid carriers to enhance antimicrobial activity. Int. J. Pharm. 526, 244–253. https://doi.org/10.1016/j.ijpharm.2017.04.071.

Li, X., Li, P., Saravanan, R., Basu, A., Mishra, B., Lim, S.H., Su, X., Tambyah, P.A., Leong, S.S.J., 2014. Antimicrobial functionalization of silicone surfaces with engineered short peptides having broad spectrum antimicrobial and salt-resistant properties. Acta Biomater. 10, 258–266. https://doi.org/10.1016/j.actbio.2013.09.009.

Li, B., Zhang, Y., Guo, Q., He, S., Fan, J., Xu, L., Zhang, Z., Wu, W., Chu, H., 2022. Antibacterial peptide RP557 increases the antibiotic sensitivity of Mycobacterium abscessus by inhibiting biofilm formation. Sci. Total Environ. 807, 151855 https://doi.org/10.1016/j.scitotenv.2021.151855.

Lim, K., Leong, S.S.J., 2018. Antimicrobial Coating Development Based on Antimicrobial Peptides. In: Handbook of Antimicrobial Coatings. Elsevier, pp. 509–532. doi: 10.1016/B978-0-12-811982-2.00022-6.

Lim, K., Chua, R.R.Y., Saravanan, R., Basu, A., Mishra, B., Tambyah, P.A., Ho, B., Leong, S.S.J., 2013. Immobilization studies of an engineered arginine-tryptophan-rich peptide on a silicone surface with antimicrobial and antibiofilm activity. ACS Appl. Mater. Interfaces 5, 6412–6422. https://doi.org/10.1021/am401629p.

Lim, K., Chua, R.R.Y., Ho, B., Tambyah, P.A., Hadinoto, K., Leong, S.S.J., 2015. Development of a catheter functionalized by a polydopamine peptide coating with antimicrobial and antibiofilm properties. Acta Biomater. 15, 127–138. https://doi.org/10.1016/j.actbio.2014.12.015.

Mataraci, E., Dosler, S., 2012. In vitro activities of antibiotics and antimicrobial cationic peptides alone and in combination against methicillin-resistant Staphylococcus aureus biofilms. Antimicrob. Agents Chemother. 56, 6366–6371. https://doi.org/10.1128/AAC.01180-12.

Mhlongo, J.T., Waddad, A.Y., Albericio, F., de la Torre, B.G., 2023. Antimicrobial Peptide Synergies for Fighting Infectious Diseases. Adv. Sci. (weinheim, Baden-Wurttemberg, Ger.) 10, e2300472. https://doi.org/10.1002/advs.202300472.

Mishra, B., Basu, A., Chua, R.R.Y., Saravanan, R., Tambyah, P.A., Ho, B., Chang, M.W., Leong, S.S.J., 2014. Site specific immobilization of a potent antimicrobial peptide onto silicone catheters: evaluation against urinary tract infection pathogens. J. Mater. Chem. B 2, 1706. https://doi.org/10.1039/c3tb21300e.

Mishra, B., Lushnikova, T., Golla, R.M., Wang, X., Wang, G., 2017. Design and surface immobilization of short anti-biofilm peptides. Acta Biomater. 49, 316–328. https://doi.org/10.1016/j.actbio.2016.11.061.

Molina, K.C., Huang, V., 2016. Resistance to non-glycopeptide agents in Serious Staphylococcus aureus infections. Curr. Infect. Dis. Rep. 18, 47. https://doi.org/10.1007/s11908-016-0553-6.

Orlando, F., Ghiselli, R., Cirioni, O., Minardi, D., Tomasinsig, L., Mocchegiani, F., Silvestri, C., Skerlavaj, B., Riva, A., Muzzonigro, G., Saba, V., Scalise, G., Zanetti, M., Giacometti, A., 2008. BMAP-28 improves the efficacy of vancomycin in rat models of gram-positive cocci ureteral stent infection. Peptides 29, 1118–1123. https://doi.org/10.1016/j.peptides.2008.03.005.

Peacock, S.J., Paterson, G.K., 2015. Mechanisms of methicillin resistance in Staphylococcus aureus. Annu. Rev. Biochem 84, 577–601. https://doi.org/10.1146/annurev-biochem-060614-034516.

Pizzolato-Cezar, L.R., Okuda-Shinagawa, N.M., Machini, M.T., 2019. Combinatory therapy antimicrobial peptide-antibiotic to minimize the ongoing rise of resistance. Front. Microbiol. 10, 1703. https://doi.org/10.3389/fmicb.2019.01703.

Rai, A., Ferrão, R., Marta, D., Vilaça, A., Lino, M., Rondão, T., Ji, J., Paiva, A., Ferreira, L., 2022. Antimicrobial peptide-tether dressing able to enhance wound healing by tissue contact. ACS Appl. Mater. Interfaces 14, 24213–24228. https://doi.org/10.1021/acsami.2c06601.

Rand, K.H., Houck, H.J., 2004. Synergy of daptomycin with oxacillin and other β-lactams against methicillin-resistant Staphylococcus aureus. Antimicrob. Agents Chemother. 48, 2871–2875. https://doi.org/10.1128/AAC.48.8.2871-2875.2004.

Reffuveille, F., de la Fuente-Núñez, C., Mansour, S., Hancock, R.E.W., 2014. A broad-spectrum antibiofilm peptide enhances antibiotic action against bacterial biofilms. Antimicrob. Agents Chemother. 58, 5363–5371. https://doi.org/10.1128/AAC.03163-14.

Shai, Y., 2002. Mode of action of membrane active antimicrobial peptides. Biopolymers 66, 236–248. https://doi.org/10.1002/bip.10260.

Sharma, A., Gaur, A., Kumar, V., Sharma, N., Patil, S.A., Verma, R.K., Singh, A.K., 2021. Antimicrobial activity of synthetic antimicrobial peptides loaded in poly-Ɛ-

caprolactone nanoparticles against mycobacteria and their functional synergy with rifampicin. Int. J. Pharm. 608, 121097 https://doi.org/10.1016/j.ijpharm.2021.121097.

Sousa, M.G.C., Xavier, P.D., Cantuária, A.P. de C., Porcino, R.A., Almeida, J.A., Franco, O.L., Rezende, T.M.B., 2021. Host defense peptide IDR-1002 associated with ciprofloxacin as a new antimicrobial and immunomodulatory strategy for dental pulp revascularization therapy. Microb. Pathog. 152 https://doi.org/10.1016/j.micpath.2020.104634.

Stepulane, A., Rajasekharan, A.K., Andersson, M., 2022. Multifunctional surface modification of PDMS for antibacterial contact killing and drug-delivery of polar, nonpolar, and amphiphilic drugs. ACS Appl. Bio Mater. 5, 5289–5301. https://doi.org/10.1021/acsabm.2c00705.

Tacconelli, E., Carrara, E., Savoldi, A., Harbarth, S., Mendelson, M., Monnet, D.L., Pulcini, C., Kahlmeter, G., Kluytmans, J., Carmeli, Y., Ouellette, M., Outterson, K., Patel, J., Cavaleri, M., Cox, E.M., Houchens, C.R., Grayson, M.L., Hansen, P., Singh, N., Theuretzbacher, U., Magrini, N., Aboderin, A.O., Al-Abri, S.S., Awang Jalil, N., Benzonana, N., Bhattacharya, S., Brink, A.J., Burkert, F.R., Cars, O., Cornaglia, G., Dyar, O.J., Friedrich, A.W., Gales, A.C., Gandra, S., Giske, C.G., Goff, D.A., Goossens, H., Gottlieb, T., Guzman Blanco, M., Hryniewicz, W., Kattula, D., Jinks, T., Kanj, S.S., Kerr, L., Kieny, M.P., Kim, Y.S., Kozlov, R.S., Labarca, J., Laxminarayan, R., Leder, K., Leibovici, L., Levy-Hara, G., Littman, J., Malhotra-Kumar, S., Manchanda, V., Moja, L., Ndoye, B., Pan, A., Paterson, D.L., Paul, M., Qiu, H., Ramon-Pardo, P., Rodríguez-Baño, J., Sanguinetti, M., Sengupta, S., Sharland, M., Si-Mehand, M., Silver, L.L., Song, W., Steinbakk, M., Thomsen, J., Thwaites, G.E., van der Meer, J.W., Van Kinh, N., Vega, S., Villegas, M. V., Wechsler-Fördös, A., Wertheim, H.F.L., Wesangula, E., Woodford, N., Yilmaz, F. O., Zorzet, A., 2018. Discovery, research, and development of new antibiotics: the WHO priority list of antibiotic-resistant bacteria and tuberculosis. Lancet Infect. Dis. 18, 318–327. https://doi.org/10.1016/S1473-3099(17)30753-3.

Tenover, F.C., Moellering, R.C., 2007. The rationale for revising the clinical and laboratory standards institute vancomycin minimal inhibitory concentration interpretive criteria for Staphylococcus aureus. Clin. Infect. Dis. 44, 1208–1215. https://doi.org/10.1086/513203.

Veyries, M.L., Couarraze, G., Geiger, S., Agnely, F., Massias, L., Kunzli, B., Faurisson, F., Rouveix, B., 1999. Controlled release of vancomycin from Poloxamer 407 gels. Int. J. Pharm. 192, 183–193. https://doi.org/10.1016/S0378-5173(99)00307-5.

Wang, S.-H., Tang, T.-W.-H., Wu, E., Wang, D.-W., Liao, Y.-D., 2020. Anionic surfactant-facilitated coating of antimicrobial peptide and antibiotic reduces biomaterial-associated infection. ACS Biomater. Sci. Eng. 6, 4561–4572. https://doi.org/10.1021/acsbiomaterials.0c00716.

Wiegand, I., Hilpert, K., Hancock, R.E.W., 2008. Agar and broth dilution methods to determine the minimal inhibitory concentration (MIC) of antimicrobial substances. Nat. Protoc. 3, 163–175. https://doi.org/10.1038/nprot.2007.521.

Wu, C.-L., Peng, K.-L., Yip, B.-S., Chih, Y.-H., Cheng, J.-W., 2021. Boosting synergistic effects of short antimicrobial peptides with conventional antibiotics against resistant bacteria. Front. Microbiol. 12, 1–10. https://doi.org/10.3389/fmicb.2021.747760.

Yeung, A.T.Y., Gellatly, S.L., Hancock, R.E.W., 2011. Multifunctional cationic host defence peptides and their clinical applications. Cell. Mol. Life Sci. 68, 2161–2176. https://doi.org/10.1007/s00018-011-0710-x.

Zarghami, V., Ghorbani, M., Pooshang Bagheri, K., Shokrgozar, M.A., 2021. Melittin antimicrobial peptide thin layer on bone implant chitosan-antibiotic coatings and their bactericidal properties. Mater. Chem. Phys. 263, 124432 https://doi.org/10.1016/j.matchemphys.2021.124432.

Zasloff, M., 2002. Antimicrobial peptides of multicellular organisms. Nature 415, 389–395. https://doi.org/10.1038/415389a.

Zharkova, M.S., Orlov, D.S., Golubeva, O.Y., Chakchir, O.B., Eliseev, I.E., Grinchuk, T.M., Shamova, O.V., 2019. Application of antimicrobial peptides of the innate immune system in combination with conventional antibiotics—a novel way to combat antibiotic resistance? Front. Cell. Infect. Microbiol. 9, 436071 https://doi.org/10.3389/fcimb.2019.00128.

Zhu, N., Zhong, C., Liu, T., Zhu, Y., Gou, S., Bao, H., Yao, J., Ni, J., 2021. Newly designed antimicrobial peptides with potent bioactivity and enhanced cell selectivity prevent and reverse rifampin resistance in Gram-negative bacteria. Eur. J. Pharm. Sci. 158, 105665 https://doi.org/10.1016/j.ejps.2020.105665.